

# Development of a Temperature Controlled Anisotropic Diffusion Phantom

C. Reischauer<sup>1</sup>, P. Staempfli<sup>1,2</sup>, T. Jaermann<sup>1</sup>, S. Kollias<sup>2</sup>, and P. Boesiger<sup>1</sup>

<sup>1</sup>Institute for Biomedical Engineering, ETH and University of Zurich, Zurich, Switzerland, <sup>2</sup>Institute of Neuroradiology, University Hospital Zurich, Zurich, Switzerland

## Introduction

Diffusion Tensor Imaging (DTI) [1] and its various applications, as e.g. fiber tracking, as well as more sophisticated, recently developed techniques such as Diffusion Spectrum Imaging (DSI) [2] and q-ball imaging [3] have gathered momentum in the MR community in the past few years. However, one main problem still arises from the lack of a gold standard to verify and to quantify the results. Particularly with regard to ongoing quantification efforts and clinical studies, quantitative comparability of results gains in importance. Diffusion phantoms establish the possibility to investigate the accuracy of diffusion parameters and especially of fiber tracking algorithms under various conditions. With phantoms, it is for instance possible to optimize diffusion weighted imaging sequences or to establish environment-independent quantities and scaling factors for multicenter studies.

In the present work, a diffusion phantom was developed which simulates fiber crossing, but as well features full temperature control in order to investigate and control temperature dependence of diffusion parameters. Therefore, diffusion weighted images were acquired over a broad temperature range and Fractional Anisotropy (FA) values as well as Apparent Diffusion Coefficients (ADCs) were measured and compared in several regions of the phantom.

## Methods

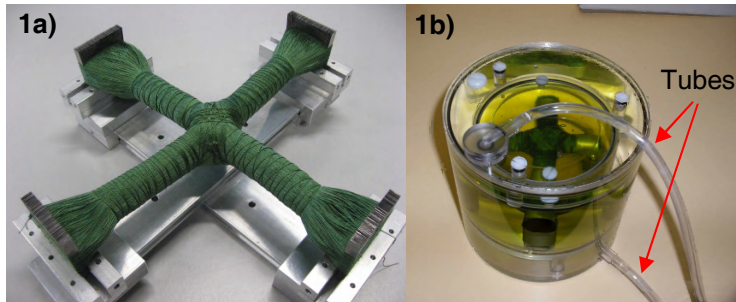


**Fig. 1:** a) Crossed woven strands mounted on the “weaving frame” and b) final phantom embedded within the heating cylinder. The two tubes (red arrows) are the inflow and outflow tubes which can be connected to a heat pump in order to circulate temperature controlled water in a closed loop.

For the phantom construction, two crossing strands of dyneema fibers ( $\varnothing$  200 $\mu$ m [4], were woven with a self constructed “weaving frame” (see fig. 1a). Each strand consisted of 2500 single dyneema fibers. The crossing area in the center of the phantom was built by systematically stacking of horizontal and parallel fiber layers of 50 fibers each. Two consecutive layers had orthogonal directions to each other. In order to achieve high fiber packing densities and consequently, high anisotropy values a single dyneema fiber was tightly wrapped around the strands at the end. Finally, the strands were cut out and mounted in a water filled cylinder with a diameter of 12 cm. To remove air bubbles within the spacing between the fibers, the phantom was degassed in a vacuum pump for several hours. The cylinder was then completely closed and fixed in the center of a bigger cylinder ( $\varnothing$  16 cm) that provided a water bath to heat up the phantom to a specific temperature by connecting it to a heat pump (see fig. 1b).

All MR acquisitions were performed on a 3 T whole-body system (Philips, Best, the Netherlands), equipped with an 8-element receive head coil array (MRI Devices Corp., Waukesha, USA). Each session consisted of 10 single-

shot spin-echo EPI DTI scans with the following parameters: Scan duration: 196 s, acquisition matrix = 96x96, reconstruction matrix = 96x96, FOV = 180x180 mm<sup>2</sup>, 25 contiguous slices, slice thickness = 1.9 mm, TE = 50 ms, NSA = 1, SENSE factor = 2.1, partial Fourier encoding = 60%, b-factor = 1000 s/mm<sup>2</sup>, 15 diffusion encoding directions. Acquisitions were performed with temperatures of 288, 293, 298, 303, 308, and 313 K. Afterwards, eddy current-induced image warping was corrected in each DTI dataset using a correlation-based registration algorithm. Finally, the 10 datasets of every temperature measurement were coregistered in order to build one mean dataset per temperature. All further calculations, as determining elements of the diffusion tensor, deriving the eigenvalues and eigenvectors, and calculating the FA as well as ADC values were performed with a dedicated software package developed in C++. FA and ADC values for each temperature value were calculated in five 3D Regions Of Interest (ROIs): four ROIs were defined in each of the four “arms” and one ROI was placed in the center of the crossing.

## Results

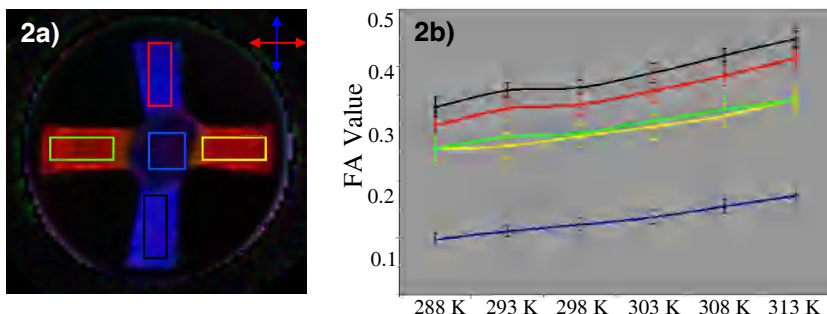


**Fig. 2:** On the left side, a slice through the center of the strands is depicted. The colors indicate the underlying fiber directions (see coordinate system in the right corner). The position of the five 3D regions of interests is illustrated by 5 colored rectangles. On the right side, the temperature dependant FA values of the 5 region of interests are shown (colors are corresponding).

Figure 2a illustrates a directionally color-coded slice through the phantom. It is clearly visible that within the strands a single direction is predominant, either left-right or bottom-up direction (cf. color coded coordinate system in the top right edge). Within the crossing, two main effects are apparent: Firstly, the anisotropy is decreased due to the special fiber architecture in this area, and secondly, there is no predominant fiber direction. The five colored rectangles depict the locations of the five 3D ROIs in which the anisotropy measurements were performed.

In figure 2b, the temperature dependent anisotropy values are depicted. The color of the five curves corresponds to the color of the ROIs in figure 2a. In all five regions, the FA values increase with increasing temperature. Moreover, a shift between the FA curves in the four “arms” of the phantom is apparent.

The course of the ADC values (not presented here) is similar to the one of the FA values, but is reversed with the highest coefficient in the central ROI and generally features fewer shifts between the curves.

## Discussion and Conclusion

The main scope of this work was to construct a diffusion phantom for quantitative analysis and comparison of diffusion parameters. Therefore, it was important to build a fully temperature controlled phantom due to the temperature dependence of the parameters. The results confirm this dependence and thus, the need to tightly control temperature. The shift between the curves (see fig. 2 b) in the four strand regions may be caused by different packing densities of the fibers due to the manual weaving and wrapping of the fibers [5].

For experimental evaluation and comparison of diffusion methods and for the development of future quantitative analyses, we believe that the phantom may become an invaluable tool to eliminate statistical bias from different hardware equipments as e.g. different manufacturers, different field strengths, and different diffusion sequences.

## References

[1] Basser PJ et al., Biophys J 1994, 66: 259-67. [2] Wedeen VJ et al., Magn Reson Med 2005, 54: 1377-86. [3] Tuch D et al., Neuron 2003, 40: 885-95. [4] Lorenz R et al., Proc. ISMRM 2006, p. 2738. [5] Fieremans E et al., Proc. ISMRM 2006, p. 1036.